JOURNAL OF VIROLOGY, Nov. 2008, p. 11084–11095 Vol. 82, No. 22
0022-538X/08/$08.00+0 doi:10.1128/JVI.01377-08

Artificial MicroRNAs Highly Accessible to Targets Confer Efficient Virus Resistance in Plants[▽]

Cheng-Guo Duan,[1,2] Chun-Han Wang,[1]† Rong-Xiang Fang,[1] and Hui-Shan Guo[1]*

State Key Laboratory of Plant Genomics and National Center for Plant Gene Research (Beijing), Institute of Microbiology, Chinese Academy of Sciences, Beijing 100101, China,[1] and Graduate University of Chinese Academy of Sciences, Beijing 100049, China[2]

Received 1 July 2008/Accepted 25 August 2008

Short-hairpin RNAs based on microRNA (miRNA) precursors to express the artificial miRNAs (amiRNAs) can specifically induce gene silencing and confer virus resistance in plants. The efficacy of RNA silencing depends not only on the nature of amiRNAs but also on the local structures of the target mRNAs. However, the lack of tools to accurately and reliably predict secondary structures within long RNAs makes it very hard to predict the secondary structures of a viral genome RNA in the natural infection conditions in vivo. In this study, we used an experimental approach to dissect how the endogenous silencing machinery acts on the 3′ untranslated region (UTR) of the *Cucumber mosaic virus* (CMV) genome. Transiently expressed 3′UTR RNAs were degraded by site-specific cleavage. By comparing the natural cleavage hotspots within the 3′UTR of the CMV-infected wild-type *Arabidopsis* to those of the triple *dcl2/3/4* mutant, we acquired true small RNA programmed RNA-induced silencing complex (siRISC)-mediated cleavage sites to design valid amiRNAs. We showed that the tRNA-like structure within the 3′UTR impeded target site access and restricted amiRNA-RISC-mediated cleavage of the target viral RNA. Moreover, target recognition in the less-structured area also influenced siRISC catalysis, thereby conferring different degrees of resistance to CMV infection. Transgenic plants expressing the designed amiRNAs that target the putative RISC accessible target sites conferred high resistance to the CMV challenge from both CMV subgroup strains. Our work suggests that the experimental approach is credible for studying the course of RISC target recognition to engineer effective gene silencing and virus resistance in plants by amiRNAs.

The mechanism of RNA silencing is that a small RNA targets a complementary mRNA for its site-specific cleavage and subsequent degradation (4, 5). RNA silencing has been used extensively to knock down genes of interest in various organisms. Small RNAs, ca. 21 to 24 nucleotides (nt) in length, are involved in the RNA silencing processes, including microRNAs (miRNAs) and other small interference RNAs (siRNAs). While siRNA duplexes can be used directly for in vitro cultures of cell lines, such as human HeLa and *Drosophila* S2 cells (32, 49, 57), stable transformation with expression cassettes producing long double-stranded RNAs or hairpin precursor RNAs is required in plants to supply substrates for RNase III-type enzymes called Dicer-like (DCL) proteins to produce siRNAs or miRNAs (3, 9, 25, 56). The small RNAs are then loaded into Argonaute protein-containing effector complexes called RNA-induced silencing complexes (RISCs). Upon recognizing a complementary mRNA, the small RNA programmed RISC (siRISC) cleaves the mRNA at a site defined by the antisense small RNA, positioned ~10 nt from the 5′ end of this guide small RNA, and the cleaved target mRNA is then degraded (24, 30, 44, 50). In addition to cleavage of target mRNA, a widespread translational inhabitation by plant miRNAs and siRNAs has recently been reported (7). To express specific miRNAs, short-hairpin RNAs based on miRNA precursor backbones (artificial miRNAs [amiRNAs]) are the most successful expression cassettes to induce highly specific gene silencing in *Arabidopsis thaliana* and in rice (1, 10, 19, 35, 37, 43, 52, 53). Potential application of amiRNAs as antiviral agents in plant biotechnology has also been reported recently (34, 38).

Over the last decade, the homology-dependent RNA-mediated silencing has widely been used to engineer antiviral resistance in plants by the expression of viral sequences in the sense or antisense orientation or in the double-stranded forms (20, 47, 54). In these cases, cosuppression of both the virus-derived transgene RNA and the invading viral RNA would occur via RNA silencing, resulting in high resistance or delayed resistance (recovery) to virus challenge (18, 27). Compared to long RNA-mediated antiviral silencing, amiRNA has several advantages for generating viral immunity. First, a long viral cDNA fragment is not required. A short amiRNA sequence without extensive homology to any plant genes can be chosen to avoid off-target effects. Second, the amiRNA-mediated approach has no environmental biosafety problem when applied in agriculture. Concerns about transforming plants with viral sequences that might complement or recombine with nontarget viruses clearly do not apply to plants expressing amiRNAs (17).

Efficient amiRNA-mediated resistance to infection with a tymovirus, *Turnip yellow mosaic virus*, and a potyvirus, *Turnip mosaic virus*, has been observed in transgenic *A. thaliana* expressing amiRNAs targeting viral mRNA sequences that encode the silencing suppressors P69 of *Turnip yellow mosaic virus* and HC-Pro of *Turnip mosaic virus* (34). However, trans-

* Corresponding author. Mailing address: State Key Laboratory of Plant Genomics and National Center for Plant Gene Research, Institute of Microbiology, Chinese Academy of Sciences, Beijing 100101, China. Phone: 86 (010) 64847989. Fax: 86 (010) 64847989. E-mail: guohs@im.ac.cn.

† Present address: Institute of Biophysics, Chinese Academy of Sciences, Beijing 100101, China.

▽ Published ahead of print on 3 September 2008.

genic tobacco plants expressing an amiRNA targeting the sequence that encodes the silencing suppressor 2b of the *Cucumber mosaic virus* (CMV) showed various degrees of responses to CMV infection, including "resistant," "recovery," "delayed infection," and "susceptible" (39). The low resistance might be due to the multiple genomes of CMV, which contain three genomic and two subgenomic RNAs. The CMV genomic RNA1 and RNA3, as well as subgenomic RNA4, are not direct targets of amiR2b, and siRNAs derived from these nontarget RNAs rapidly accumulate in plant cells, which may lead to saturation of siRISC and impair amiR2b antiviral efficacy. It may also be possible that the amiR2b target site is not in the optimal siRISC-target recognizing region.

It is generally recognized that not all siRNA species against a given mRNA target are equally effective. The efficacy of RNA silencing depends not only on the nature of siRNAs but also on the local structures of the target mRNAs (31, 36, 42). Engineered *Plum pox virus* (PPV) chimeras bearing endogenous functional miRNA target sequences that impair viral infectivity have been reported (46). The deleterious effect on virus infectivity also depends on the site of insertion of the miRNA target sequence in the viral genome, indicating that some sites are more accessible than others to the miRNA-RISC-mediated cleavage. Moreover, Simon-Mateo and Garcia (46) have also studied the stability of the PPV chimeric genome and found selections of virulent mutants in the plants infected with the PPV chimeras. These mutants contain mutations within the miRNA target sequence that mainly affect nucleotide matching to the 5′-terminal region of the miRNA, indicating that virus can readily evolve to escape the amiRNA-mediated silencing mechanism under the negative pressure of miRNA activity (46).

Target site accessibility that can influence siRNA-programmed RISC catalysis has been analyzed by biochemical and bioinformatics approaches in animal cell lines (2, 8, 45). Computational modeling of the secondary structure of a target and assessment of the effect of secondary structure on target accessibility can be predicted via bioinformatics methods. However, the major drawback for diverse applications of siRNA-mediated target RNA cleavage in medicine and in agriculture is the lack of tools to accurately and reliably predict secondary structures within long RNAs that are adopted in their native conditions in vivo since an mRNA is unlikely to have a single stable structure.

CMV is one of the best-characterized tripartite positive-sense single-stranded RNA viruses (48), and it can be divided into three subgroups: IA, IB, and II (41). High nucleotide sequence similarity is present within the 3′ untranslated region (3′UTR) of multiple RNA genomes of CMV, and the homology in the 3′UTR sequences is extensive among the three genomes and the two subgenomes. The similarities between the 3′UTR are even more apparent when secondary structures are considered since they can all be base paired to form a tRNA-like structure (TLS) (26, 40). It has been shown that the TLS segment contains the promoter for minus-strand synthesis of the viral RNA during replication, and the primary function of the TLS is to interact with the replicase (e.g., the 1a and 2a proteins encoded by RNA1 and -2, respectively) and other host factors (15). The importance of the 3′UTR in CMV replication and the high stability of nucleotide sequence and three-dimensional structures of TLS prompt us to explore antiviral activity using 3′UTR-based amiRNA-mediated RNA silencing.

In the present study, we used an experimental approach to analyze the effect of target site accessibility and to engineer effective anti-CMV silencing in plants by amiRNAs. We compared the natural cleavage hot spot sites within the 3′UTR of the CMV-infected wild-type *Arabidopsis* to those of the triple *dcl2/3/4 Arabidopsis* mutant. In the triple *dcl* mutant, three of the four DCL proteins, DCL2, DCL3, and DCL4, which show hierarchical antiviral activities in addition to their endogenous function in *Arabidopsis*, are mutated, and only DCL1 may be functional for processing hairpin RNAs in the miRNA pathway (6, 12, 16, 33, 51, 58). Moreover, with the plant transient-expression assay, potential DCL- and RISC-mediated cleavage sites in the viral RNA were evaluated under natural viral infection conditions. We found that transgenic plants expressing amiRNAs that target the putative DCL-mediated cleavage sites, such as those in the TLS region, showed no protection against CMV infection. However, both transgenic *Arabidopsis* and tobacco expressing amiRNAs that target the putative RISC accessible sites conferred a high resistance to CMV challenge from both subgroup strains. amiRNAs were also expressed in transgenic plants carrying a polymeric amiRNA precursor, which ligated three amiRNA monomers into a single transcription unit; these plants also conferred high resistance to CMV infection.

MATERIALS AND METHODS

Construction of artificial pre-amiRNAs. The *Arabidopsis* pre-miR159a sequence was used as a backbone for the construction and expression of amiRNAs as described previously (34). Using oligonucleotide-directed mutagenesis, the mature miR159 sequence was replaced with the synthetic sequences, each corresponding to a designed amiRNA. The amiRNA primers were designed as below. The forward primers are: amiR-Q-1 (5′-*AGATCT*TGATCTGACGATGGAAGCTTCGTGAGAACATCGTGCACCATGAGTTGAGCAGGGTA-3′), amiR-Q-2 (5′-*AGATCT*TGATCTGACGATGGAAGTCGTGTCTTTCTAACGCCGATCATGAGTTGAGCAGGGTA-3′), amiR-SD-1 (5′-*AGATCT*TGATCTGACGATGGAAGGGTTTCTTCGGTCGGACTTCGCATGAGTTGAGCAGGGTA-3′), amiR-SD-2 (5′-*AGATCT*TGATCTGACGATGGAAGTCGTGGAGAAAAACACGCCAGCATGAGTTGAGCAGGGTA-3′), amiR-SD-3 (5′-*TCTAGATCT*TGATCTGACGATGGAAGGGCTAAAATGGAAAGTCGTGGCATGAGTTGAGCAGGGTA-3′), amiR-SD-4 (5′-*AGATCT*TGATCTGACGATGGAAGCACTAAACGCTAGGCGGTGAACATGAGTTGAGCAGGGTA-3′), and amiR-SD-5 (5′-*TCTAGATCT*TGATCTGACGATGGAAGTACAAACTGTCATAAGTCACTCATGAGTTGAGCAGGGTA-3′). The forward primers contain BglII site (indicated in italics) and the amiRNA* sequence (underlined). The amiR-SD-3 and amiR-SD-5 forward primers also an contain XbaI site (in italics). The reverse primers contain the mature amiRNA reverse complementary sequence (underlined), and they are as follows: amiR-Q-1 (5′-GCTTCGTGAGAAGCTCGTGCACGAAGAGTAAAAGCCATTA-3′), amiR-Q-2 (5′-GTCGTGTCTTTCACACGCCGATGAAGAGTAAAAGCCATTA-3′), amiR-SD-1 (5′-GGGTTTCTTCGGAAGGACTTCGGAAGAGTAAAAGCCATTA-3′), amiR-SD-2 (5′-GTCGTGGAGAAATCCACGCCAGGAAGAGTAAAAGCCATTA-3′), amiR-SD-3 (5′-GGGCTAAAATGGTCAGTCGTGGGAAGAGTAAAAGCCATTA-3′), amiR-SD-4 (5′-GCACTAAACGCTTTGCGGTGAAGAAGAGTAAAAGCCATTA-3′), and amiR-SD-5 (5′-GTACAAACTGTCTGAAGTCACTGAAGAGTAAAAGCCATTA-3′).

amiRNA precursor PCR DNA fragment was ligated into pGEM-T vector and cloned into binary vector pCAMBIA-1300221 to generate pCAMBIA-pre-amiRNA, in which pre-amiRNAs are placed downstream of the 35S promoter.

To obtain amiR-SD-2/3/5 precursor, an XbaI-SpeI fragment of pGEM-T-pre-amiR-SD-3 was inserted into SpeI-digested 35S-pre-amiR-SD-2, giving 35S-pre-amiR-SD-2/3. An XbaI-SpeI fragment of pGEM-T-pre-amiR-SD-5 was inserted into SpeI-digested 35S-pre-amiR-SD-2/3 and generated 35S-pre-amiR-SD-2/3/5.

Construction of CMV subgenomic RNAs and β-glucuronidase (GUS)-sensor. Plasmid pQCD1 containing the cDNA clone of Q-CMV RNA1 (13) was digested with XhoI-BamHI, a 962-nt fragment corresponding to the 3′ termini of Q-CMV

RNA1 was cloned into pCAMBIA-1300221 to generate 35S-R1*. Q-CMV subgenomic RNA4A and RNA4 sequences were amplified by PCR using pQCD2 and pQCD3 (which contain the cDNA clones of Q-CMV genomic RNA2 and RNA3, respectively) (13) as templates, respectively. The forward primers QR4-5 (5′-*TCTAGA*AGCGTTTAGTTGTTCACCTG-3′) and QR4A-5 (5′-*TCTAGA*GTTTTGTATATCTGAGTTCC-3′) contain the XbaI site (indicated in italics). The reverse primers QR4-3 (5′-*GAGCTC*TGGTCTCCTTATGGAGAAC-3′) and QR4A-3 (5′-*GAGCTC*TGGTCTCCTTATGGAGAACC-3′) contain the SacI site (indicated in italics). The XbaI-SacI fragments were cloned into XbaI/SacI-digested pCAMBIA-1300221, giving 35S-R4 and 35S-R4A.

A GUS-sensor construct, in which the GUS was fused to the amiR-Q-1 target sequence, was created by PCR amplification. pCAMBIA-1300221 was used as a template, and a pair of primers was designed to amplify a 426-bp fragment of the 3′ terminus of the GUS-amiR-Q-1 target sequence (GUS-sensor fragment). The forward primer GUS-sensor-5 (5′-*TGTACA*GCGAAGAGGCAGTC-3′) contains the BsrGI site (indicated in italics) and the reverse primer GUS-sensor-3 (5′-*TGTACA*GTGCACGAGCTTCTCACGAAGTTGAGTGCAGCCCGGCTAAC-3′) contains the BsrGI site (indicated in italics) and introduced a 21-nt sequence (underlined) complementary to 2105 to 2125 nt of the Q-CMV RNA3, a region corresponding to cleavage hot spot sites obtained from the 35-R4 infiltration assay. The generated GUS-sensor fragment was digested with BsrGI and replaced the corresponding GUS 3′-terminus sequence in pCAMBIA-1300221, giving 35S-GUS-sensor.

Plant transformation and virus inoculation. *Arabidopsis* transformation was carried out by the floral dip method (11) and tobacco transformation by coculture with *Agrobacterium tumefaciens*. The selective medium contained MS medium plus hygromycin 20 mg/liter. Leaves of 4-week-old *Arabidopsis* and tobacco plants were infected with a fresh sap prepared from CMV-infected tobacco leaves (1 g of ground leaf material diluted into 5 ml of phosphate buffer). All plants examined in the present study were continuously monitored over the whole experiment (about 2 months).

5′RLM-RACE assay. The 5′RACE (rapid amplification of cDNA ends) assay was performed by using the First Choice RLM-RACE kit (Ambion). Portions (2 μg) of total RNAs were used for direct ligation to the 5′RACE RNA adapter, and subsequent steps were done according to the manufacturer's directions. PCR fragments obtained from 5′RACE were cloned into the pGEM-T vector (Promega), and individual clones were selected for DNA sequencing.

Northern blot hybridizations. Total RNA was isolated from plant tissues using TRIzol reagent (Invitrogen) according to the manufacturer's instructions. For high-molecular-weight RNA blots, 10 μg of total RNA was loaded. [α-^{32}P]dCTP-labeled cDNA probes specific for the respective RNA were used. For low-molecular-weight RNA blots, 30 μg of total RNA was loaded. [α-^{32}P]UTP-labeled transcript or [γ-^{32}P]ATP-labeled specific oligonucleotide probe sequences was used.

ELISA detection of virus accumulation. Enzyme-linked immunosorbent assay (ELISA) was carried out using a polyclonal antiserum to the Q-CMV or SD-CMV coat protein (CP). Polyclonal antiserum to SD-CMV CP was also used in the detection of Fny-CMV CP because of the high identity (98.2%) of amino acid sequences between the SD-CMV and Fny-CMV CP. Readings were taken 1 h after substrate hydrolysis.

RESULTS

Determination of target recognition in the 3′UTR of CMV for the endogenous silencing machinery. To investigate how the 3′UTR of CMV genome is targeted by the endogenous silencing machinery, we constructed a full-length subgenomic RNA4 from CMV Q strain (Q-CMV, subgroup II). This construct contained an open reading frame encoding the CP and the full 3′UTR sequence (named 35S-R4) and was used for transient expression in *Nicotiana benthamiana* leaves. Northern blot analysis of small RNAs extracted from the infiltrated leaves showed that the host silencing machinery possibly targeted RNA4, resulting in the accumulation of the 3′UTR-derived siRNAs (vsiRNAs) (Fig. 1). The expression of RNA4 was readily detectable at 2 days postinfiltration (dpi) (Fig. 1) but decreased at 3 to 4 dpi. Interestingly, at 4 dpi, there was a significant increase in the hybridization signal of ~100 bp (Fig. 1), suggesting that the decrease in RNA4 might result from the

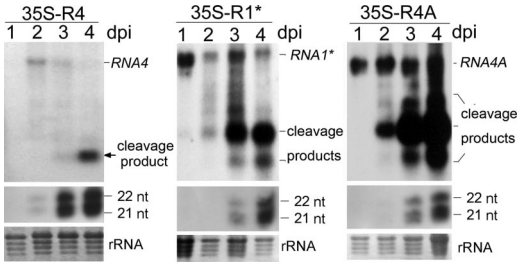

FIG. 1. Site-specific cleavage of transient expression of Q-CMV RNAs. Northern blot analysis of transient expression of Q-CMV RNAs (RNA4, RNA1*, and RNA4A) in *N. benthamiana* infiltrated with 35S-R4, 35S-R1*, or 35S-R4A. ^{32}P-labeled DNA probes specific for the full-length 3′UTR of each corresponding Q-CMV genome RNAs were used. The specific cleavage product is indicated. ^{32}P-labeled transcript probes specific for each corresponding 3′UTR were used for detection of the 3′UTR-derived siRNAs. RNA loading was monitored by methylene blue staining of the rRNA.

cleavage of RNA4 at certain regions or points that excelled the 3′UTR-derived siRNA-mediated random degradation of RNA4. Coinfiltration experiments with combinations of the target RNA and small RNA indicated that cleavage of RNA4 was likely to have been mediated by DCLs (see second section of Results and Fig. 3). Similar site-specific cleavage was observed from the transient expression of CMV subgenomic RNA4A (encoding the 2b protein) and the 3′ terminus of genomic RNA1 (encoding part of the 1a protein), both containing the full 3′UTR sequence (named as 35S-R4A and 35S-R1*, respectively; Fig. 1).

To determine the cleavage sites of RNA4, the region downstream of the 3′UTR was selected to design outer and inner primers for 5′RACE assays (Fig. 2A). A specific 5′RACE PCR band was obtained from *N. benthamiana* leaves infiltrated with 35S-R4. Sequencing of nine 5′RACE PCR clones showed that the cleavage sites were located at nt 241 to 242 (3/9) and nt 242 to 243 (6/9) (Fig. 2A, hollow red arrows), which are inside the TLS region. To investigate whether the cleavage sites represent the natural targeted sites of the 3′UTR in the CMV-infected plant cells by the silencing machinery, 5′RACE was performed with samples derived from *N. glutinosa* infected with Q-CMV. Sequencing results of 19 clones from the specific 5′RACE PCR products showed that only 2 of the 17 cleavage sites (Fig. 2A, solid red arrows) were located at the TLS region, and these did not overlap with the sites identified in the infiltration assay, suggesting that the cleavage event in a natural virus infection is diverse and complex. Most of the 15 cleavage sites that mapped outside the TLS region were located at nt 130 to 150 (8/15), forming a cleavage hot spot (Fig. 2A, solid red arrows). Therefore, in a natural infection, the effective target recognition hot spot sites for the endogenous silencing machinery are likely outside the TLS region.

Cleavage was also determined in *Arabidopsis* infected with the severe field CMV ShanDong strain (SD-CMV, subgroup IB). From the sequences of 31 clones obtained from specific 5′RACE PCR bands, 28 different cleavage sites were detected, and all were upstream of the TLS. Twelve of these formed a cleavage hot spot (nt 143 to 167) similar to that found in the Q-CMV 3′UTR (Fig. 2A, solid black arrows). To avoid disturbance of most DCL-mediated cleavage sites and to uncover

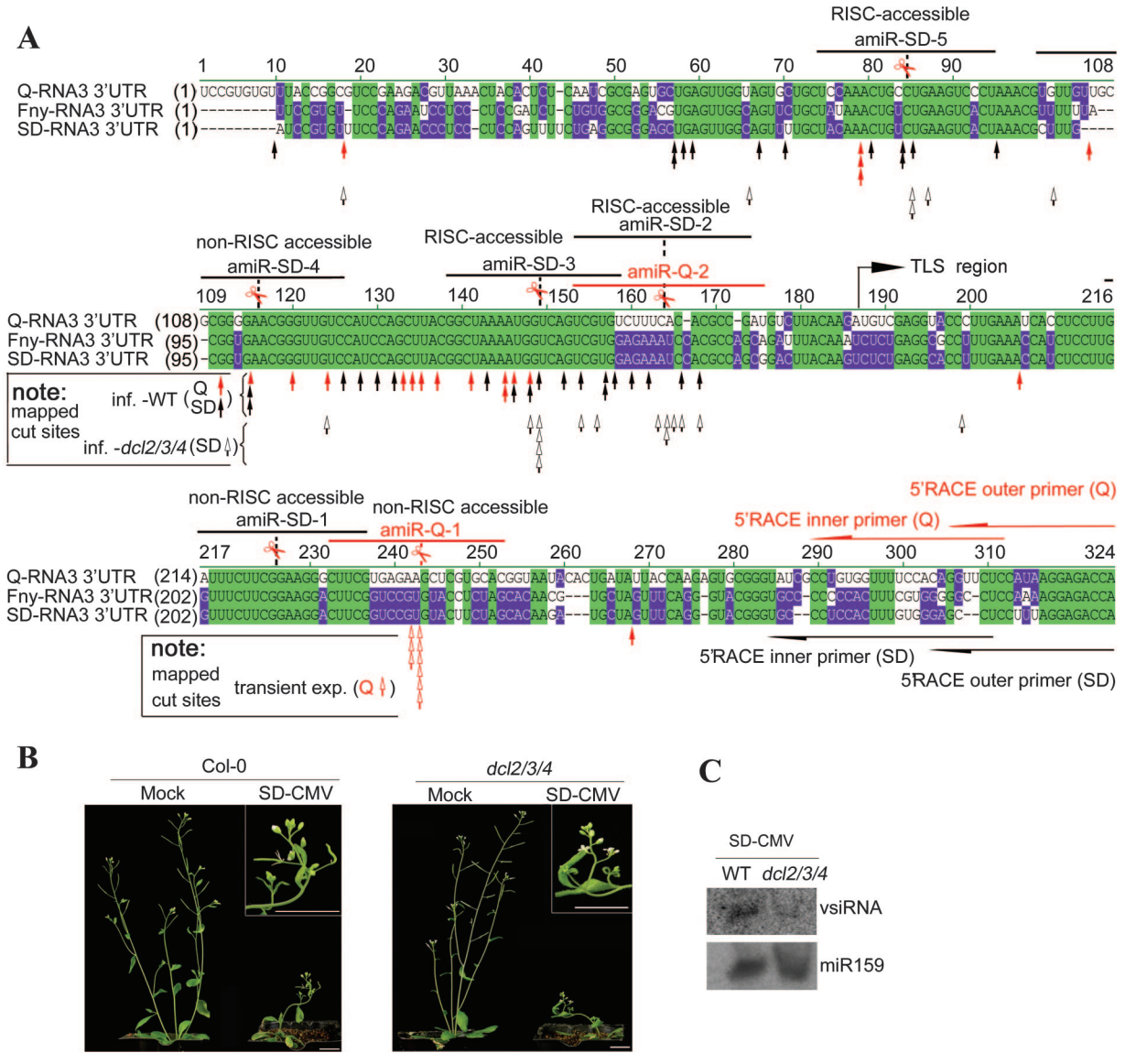

FIG. 2. Mapping of the cleavage sites of the 3′UTR RNA and analysis of the 3′UTR-derived siRNAs. (A) Mapping of the cleavage site of the 3′UTR of CMV genomic RNA3 by 5′RACE. An alignment of each of the RNA3 3′UTRs of three CMV strains is shown. Identical nucleotides within the three strains and any two strains are highlighted in green and purple, respectively. The TLS region is indicated. Outer and inner primers specific for Q-CMV (red) and SD-CMV (black) for 5′RACE are labeled. Mapped cleavage sites are indicated with hollow red arrows (from transient expression of 35S-R4), solid red arrows (from Q-CMV-infected *N. glutinosa*), solid black arrows (from SD-CMV-infected wild-type *Arabidopsis*), and hollow black arrows (from SD-CMV-infected triple *dcl2/3/4* mutant *Arabidopsis*). amiRNAs specifically targeting Q-CMV and SD-CMV 3′UTR sequences are marked with red and black lines, respectively, above the aligned sequences. Putative target accessibility is labeled with RISC-accessible or non-RISC-accessible above the given amiRNAs. (B) Similar developmental defects caused by SD-CMV infection in *Arabidopsis* wild-type Col-0 and *dcl2/3/4* mutant and infection symptoms in influorescences (inset) are shown. Photographs were taken at 20 days postinfection. (C) Northern blot analysis of the 3′UTR-derived siRNA accumulation in the SD-CMV-infected wild-type or triple *dcl2/3/4* mutant *A. thaliana*. ^{32}P-labeled specific oligonucleotide probe sequences (a mixture) complementary to the 3′UTR regions were used. The membrane was stripped and rehybridized with miR159 as a loading control.

sites being cleaved more efficiently and possibly mediated by siRNAs-RISC, *Arabidopsis* triple *dcl* mutant plant (*dcl2/3/4*) were infected with SD-CMV (Fig. 2B). Systemic infected leaves were first collected to determine the 3′UTR-derived vsiRNAs. vsiRNAs were detected at a very low level in the SD-CMV-infected *dcl2/3/4* mutant compared to the wild-type plant (Fig. 2C). The low-level vsiRNAs detected in the infected *dcl2/3/4* mutant suggested that they might produce by DCL1 or by residual activity of the mutated DCLs, if one or more DCLs were not null mutants. Fifteen of the sixteen cleavage sites from the 21 5′RACE clones were upstream of the TLS, and only one cleavage site was located in the TLS region (Fig. 2A, hollow black arrows). Nine cleavage sites in the *dcl2/3/4* mutant overlapped with the cleavage hot spot region found in the wild-type plant infected with SD-CMV. Although we could not rule out that these cleavage sites, particularly the one within

the TLS region, might be mediated by DCL1, the cleavage sites located within the less-structured 5′-terminal region of 3′UTR suggest that they are likely mediated by RISC, programmed by a low level of vsiRNAs. We also could not rule out that some of the mapped cleavage sites might result from random RNA degradation. Nevertheless, this result suggests that target recognition hotspots for the endogenous silencing machinery in the CMV 3′UTR are upstream of the TLS region in both wild-type and triple *dcl* mutant *Arabidopsis*. Based on these data, we could select valid target sites more reasonably for designing the artificial miRNAs described below.

Designing and transient expression of amiRNAs and amiRNA-mediated cleavage of target RNAs. The preferred putative siRISC cleavage site in the SD-CMV 3′UTR was between nt 148 and 149 (nt 148/149) (Fig. 2A) in the cleavage hot spot, where cleavage was detected one and four times in the wild type and *dcl2/3/4* mutant, respectively. A U nucleotide at the position immediately after the cleavage site is also consistent with the endonuclease-preferred slicing position found in most miRNA-mediated cleavage of target mRNAs (22, 39). Sequence alignment showed that the amiRNA targeting area was highly conserved in the 3′UTR regions of all three SD-CMV genome RNAs (data not shown). Moreover, the sequence was also conserved in the three genome RNAs of Fny-CMV (a subgroup IA strain) and Q-CMV RNA3, but it differed by 5 nt in Q-CMV RNA1 and RNA2 (data not shown). This amiRNA is referred to as amiR-SD-3 (Fig. 2A).

The second amiRNA (amiR-SD-2) was designed to target the cleavage site at nt 163 and 164, which was detected twice in the *dcl2/3/4* mutant (Fig. 2A). Sequence alignment showed that the amiR-SD-2 target sequence was highly conserved in the 3′UTR of all three genome RNAs in SD- and Fny-CMV but not in Q-CMV (Fig. 2A). Therefore, we designed amiR-Q-2 to specifically target the same area of the 3′UTR in Q-CMV (Fig. 2A).

amiR-SD-5 was designed to target the 3′UTR region that was conserved in the three CMV strains with the cleavage site (nt 84/85), detected once and twice in the wild type and *dcl2/3/4* mutant, respectively (Fig. 2A).

For the control, we designed amiR-SD-4 to target an area (nt 115/116) that was not in the cleavage hot spot but was still quite conserved in the 3′UTR of different CMV strains (Fig. 2A), and amiR-Q-1 was designed to target the TLS region, which contains the cleavage sites (nt 241/242 and nt 242/243) that were detected three and six times with transient expression samples; this cleavage seemed to be mediated by DCLs but not by siRNA-RISC (see below). Since the target area sequence of amiR-Q-1 was not conserved among Q-, SD-, and Fny-CMV, we also designed an amiR-SD-1 that is adjacent to the target area of ami-Q-1 to target the area in the TLS region that is conserved in all three CMV strains (Fig. 2A).

Because *Arabidopsis* miRNA precursor *MIR159a* has been shown to be effective in expressing artificial miRNAs (34), we chose *Arabidopsis* pre-miR159a as a backbone for the construction and expression of amiRNAs. Using oligonucleotide-directed mutagenesis, we replaced the 21-nt sequence of miR159 with the synthetic sequences, each corresponding to an amiRNA named pre-amiR-SD-1, -2, etc. Transient expression of each amiRNA was confirmed by Northern blot analysis (data not shown). To create a high level of resistance to CMV, particularly to the severe field strains, we constructed a polymeric amiRNA precursor by ligating pre-amiR-SD-2, pre-amiR-SD-3, and pre-amiR-SD-5 and by expressing the polymer in a single transcription unit under the 35S promoter; this construct was named 35S-amiR-SD-2/3/5. Transient expression of each amiRNA was confirmed by Northern blot analysis (data not shown).

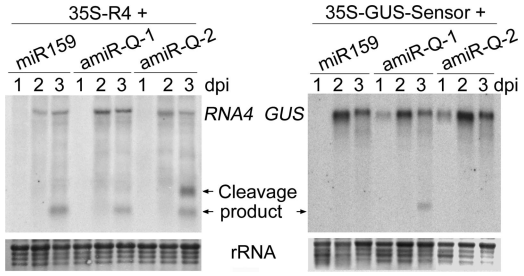

FIG. 3. Analysis of amiRNA-mediated cleavage of the target RNAs by a transient assay. Northern blot analysis of transient expression of RNAs in *N. benthamiana* coinfiltrated with 35S-R4 or GUS-sensor construct with one of the pre-amiRNAs as indicated on the top of panels. ^{32}P-labeled DNA probes specific for the full-length 3′UTR of Q-CMV RNA4 or GUS mRNA were used, respectively. Specific cleavage products are indicated.

amiRNA-mediated cleavage of the target RNAs was confirmed by coinfiltrating *N. benthamiana* leaves with agrobacterial cells carrying plasmids containing the target constructs and the proper pre-amiRNAs (Fig. 3, left panel, and data not shown). Figure 3 shows amiR-Q-2-mediated cleavage of the target RNA4 transcript. An additional hybridization signal was specifically detected with the coinfiltration of 35S-R4 with amiR-Q-2, compared to the coinfiltration of 35S-R4 with amiR-Q-1, in which the hybridization signals were similar to those observed with 35S-R4 infiltration alone (Fig. 1) or with coinfiltration of pre-miR159a (Fig. 3, left panel). To examine whether the synthetic amiR-Q-1 was biologically functional, a GUS-sensor construct, in which the GUS was fused to the amiR-Q-1 target sequence, was coinfiltrated into *N. benthamiana* with amiR-Q-1 or amiR-Q-2. Northern blot analysis showed that amiR-Q-1 could mediate cleavage of the GUS-sensor RNA (Fig. 3, right panel), indicating that the synthetic amiR-Q-1 was biologically functional but simply not able to program RISC-mediated cleavage of RNA4. This result revealed that the amiR-Q-1 target site, which was located in the TLS region, was not accessible by siRNA-RISC. Without complementary sequences between the GUS-sensor and amiR-Q-2, amiR-Q-2 did not mediate cleavage of the GUS-sensor RNA. This result also indicated that there was no endogenous siRNA-mediated cleavage of GUS-sensor RNA at the amiR-Q-1 target site, suggesting that the cleavage product detected in the 35S-R4 infiltration assay (Fig. 1A) did not result from endogenous siRNA-mediated cleavage but that it probably derived from DCL-mediated cleavage at the TLS region.

Specificity of amiRNAs in transgenic plants. Constructs of 35S-amiR-SD-1, -2, -3, -4, -5, and -2/3/5 were transformed into both *A. thaliana* (Columbia) and *Nicotiana tabacum* (*Xanthi-nc*); 35S-amiR-Q-1 and -2 were transformed into tobacco only since Q-CMV does not cause clear disease symptoms in *Arabidopsis*.

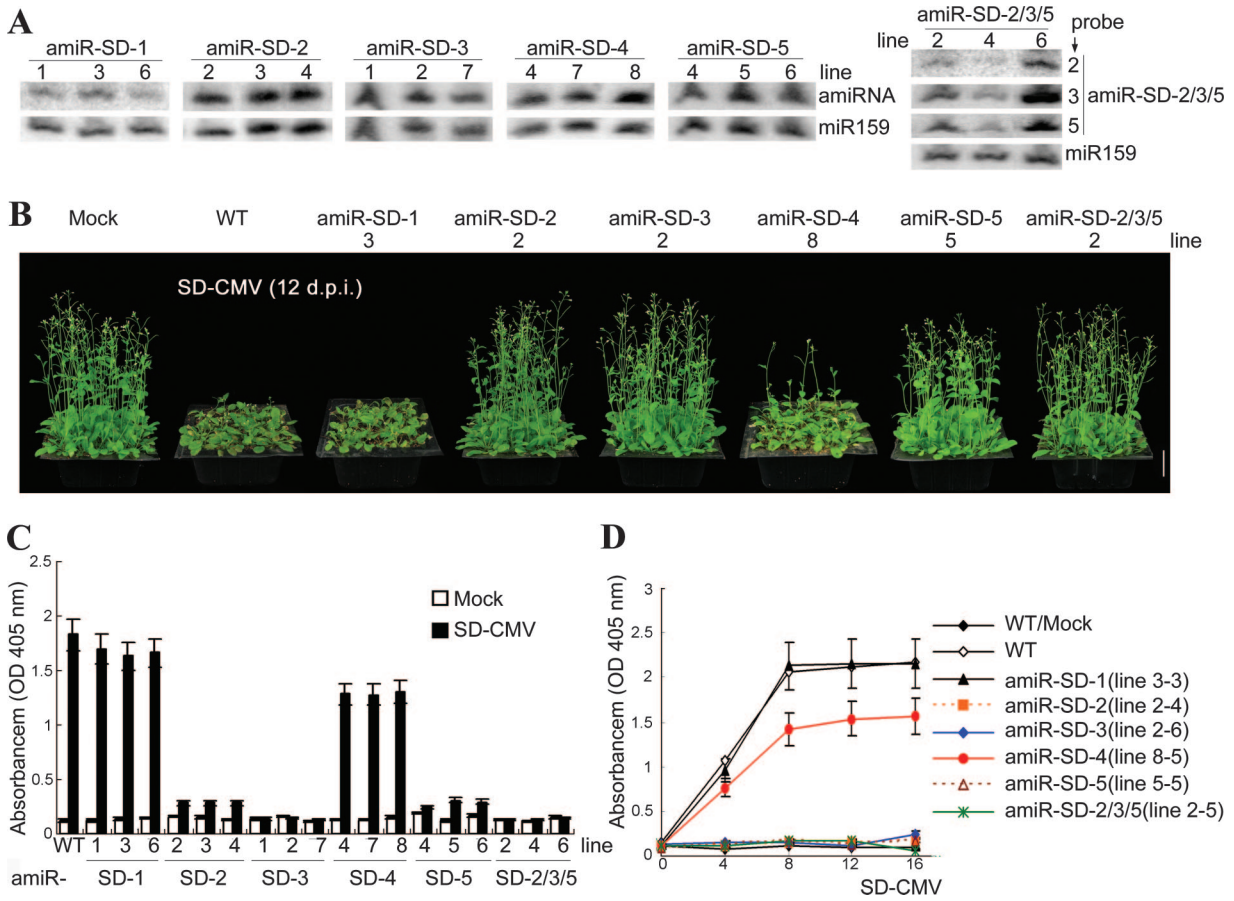

FIG. 4. Analysis of resistance to SD-CMV infection in the transgenic *A. thaliana* plants expressing amiRNAs. (A) Detection of amiRNA expression levels in three independent lines of transgenic T2 progeny plants carrying 35S-amiR-SD-1, -2, -3, -4, -5, and -2/3/5. The miR159 was used as a loading control. Line numbers are indicated on the top. (B) Transgenic T2 progeny plants were inoculated with SD-CMV and photographs were taken at 12 dpi, one representative line (indicated on top) of each genotype plants is shown. Bar, 3 cm. (C) ELISA detection of SD-CMV CP in upper noninoculated leaves of SD-CMV inoculation plants at 16 dpi. Bars represent the standard deviations ($n = 12$). (D) Time course of SD-CMV titer in upper leaves of various transgenic T3 homozygote lines (as labeled) and wild-type plants at 0, 4, 8, 12, and 16 dpi. Bars show the standard deviations ($n = 12$).

We verified the expression of each amiRNA in the transgenic lines (Fig. 4A, 6A, and data not shown).

Using a BLAST search, we failed to find any *Arabidopsis* genes that are complementary for more than 15 nt over the 21-nt sequences of our amiRNAs. To further eliminate the possibility that the amiRNAs would target endogenous mRNAs, we searched against the TIGR tobacco and *Arabidopsis* mRNA databases for potential targets for our amiRNAs using the miRU program (http://bioinfo3.noble.org/miRNA/miRU.htm). There was one *Arabidopsis* transcript (At3g 29250) that could potentially form an imperfect pairing (mismatch and deletion) with amiR-SD-3 when three mismatches are allowed (Fig. 5). Semiquantitative reverse transcription-PCR analysis of the At3g29250 transcript level in the wild-type and amiR-SD-3 transgenic *Arabidopsis* confirmed that this gene was not downregulated in the amiR-SD-3 transgenic plant (Fig. 5), suggesting that the putative target gene was not affected by the amiR-SD-3. With TIGR Tobacco Gene Index 1, there were no putative targets identified for the amiRNAs when three mismatches were allowed; however, we cannot exclude the possibility that genes that have not yet been identified could be potential targets.

Nevertheless, all transgenic plants expressing the amiRNAs displayed normal morphology and growth rates. There was no difference in flowering time or fertility compared to wild-type plants. Moreover, the expression level of the endogenous miR159 was unaltered in all of the transgenic plants compared

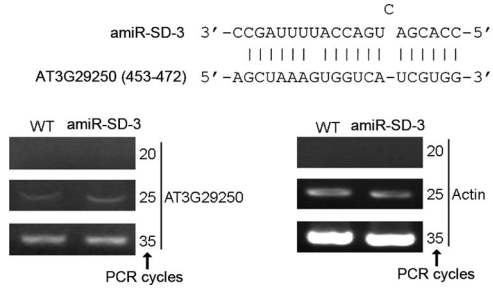

FIG. 5. Transcript analysis of the predicted target gene (AT3G29250) of amiR-SD-3 in wild-type and amiR-SD-3 transgenic *A. thaliana* by semiquantitative reverse transcription-PCR. Endogenous actin transcript was used as a control. PCR amplification cycles are indicated. The AT3G29250 transcript/amiR-SD-3 pair containing three mismatches in base pairing is shown.

TABLE 1. Infectivity assay of amiRNA transgenic *Arabidopsis* challenged with SD-CMV

Transgenic plant	Infected/total inoculated plants[a]					
	Expt 1			Expt 2		
	Line	I/T	R (%)	Line	I/T	R (%)
amiR-SD-1	1	12/24	8.3	1-3	14/16	12.5
	3	24/24	0	3-3	16/16	0
	6	24/24	0	6-7	15/16	6.25
amiR-SD-2	2	0/24	100	2-4	0/16	100
	3	2/24	91.7	3-5	0/16	100
	4	2/24	91.7	4-8	0/16	100
amiR-SD-3	1	0/24	100	1-7	0/16	100
	2	0/22	100	2-6	0/16	100
	7	0/24	100	7-4	0/15	100
amiR-SD-4	4	18/24	25	4-7	10/14	28.6
	7	16/24	33.3	7-11	12/16	25
	8	20/24	16.7	8-5	13/16	18.8
amiR-SD-5	4	4/24	83.3	4-2	0/15	100
	5	2/24	91.7	5-5	0/15	100
	6	0/24	100	6-1	0/16	100
amiR-SD-2/3/5	2	0/24	100	2-5	0/16	100
	4	0/24	100	4-4	0/16	100
	6	0/24	100	6-2	0/16	100
Wild type		26/27	3.7		26/28	7.1

[a] Wild type and three lines of T2 progeny transgenic plants of each genotype in experiment 1 and T3 progeny transgenic plants (homozygotes) in experiment 2 were inoculated with SD-CMV. I/T, The nominator (I) indicates the number of ELISA-positive plants displaying SD-CMV-infected symptoms, and the denominator (T) indicates the total number of inoculated plants. R, number of resistant plants as a percentage of the total inoculated plants.

to wild-type plants (data not shown), suggesting that the expression of amiRNAs in vivo using the pre-miR159a sequence as a backbone has little effect on the expression of endogenous miR159.

CMV resistance of transgenic *Arabidopsis*. SD-CMV causes severe disease symptoms in *Arabidopsis* ecotype Columbia, including stunting, reduced internodal distances, curly inflorescence, and snaky siliques (Fig. 2B) (14). Wild-type and three independent lines of each transgenic amiRNA *Arabidopsis* (T2 progeny, including homozygotes and hemizygotes) were challenged with sap extracted from SD-CMV-infected tobacco plants (Table 1, experiment 1). At 12 days postinoculation, typical disease symptoms were observed in 26 of 27 wild-type plants, in all plants from two amiR-SD-1 lines (lines 3 and 6) and in 22 of 24 plants of the amiR-SD-1 line 1 (Fig. 4B and Table 1). Most plants of the amiR-SD-4 lines (18, 16, and 20 out of 24 of lines 4, 7, and 8, respectively) were susceptible to SD-CMV infection. In contrast, all plants from the three amiR-SD-3 lines (lines 1, 2, and 7) did not show any apparent disease symptom (Fig. 4B and Table 1). Similar results were also obtained from all plants of the three polymer amiR-SD-2/3/5 lines (lines 2, 4 and 6), which showed 100% resistance to SD-CMV. amiR-SD-2 lines (lines 2, 3, and 4) and amiR-SD-5 lines (lines 4, 5, and 6) were clearly protected against SD-CMV infection with resistance levels ranging between 91.7 and 100% and between 83.8 and 100%, respectively (Fig. 4B and Table 1).

ELISAs were performed to detect SD-CMV CP in extracts from the systemic leaves of individual inoculated plants at 16 dpi. SD-CMV CP was undetectable in all inoculated plants of the amiR-SD-3 and amiR-SD-2/3/5 lines and in the plants without symptoms of the amiR-SD-2 and amiR-SD-5 lines, confirming virus resistance. In contrast, SD-CMV CP accumulated at high levels in wild type, amiR-SD-1 and amiR-SD-4 plants displaying virus symptoms (Fig. 4B). The average ELISA readings for each line are shown in Fig. 4C.

A second experiment was performed to monitor the development of disease symptoms and SD-CMV CP accumulation in the T3 progeny (homozygotes) plants of all genotypes. Most plants from the amiR-SD-1 lines were highly susceptible to SD-CMV infection just like the wild-type plants (Table 1). A low level of resistance was also found for the amiR-SD-4 plants (18.8 to 28.6%), similar to the results from the T2 plants. However, T3 progenies of all amiR-SD-2, -3, -5, and -2/3/5 lines were 100% resistant to SD-CMV. Figure 4D shows a course ELISA with the average readings from plants derived from one line of each genotype. Together, these results indicate that amiR-SD-2, -3, and -5, but not amiR-SD-4 and amiR-SD-1, can confer a high level of resistance to SD-CMV infection. Among the single constructs, amiR-SD-3, whose targeting area is in the cleavage hot spot mediated by siRNA-RISC (Fig. 2A), is likely to be the best amiRNA for conferring resistance to SD-CMV infection. Consistent with this result, the polymer amiR-SD-2/3/5 also conferred the highest resistance to infection (Table 1). Our results also showed that the resistance trait can be transmitted to the next generation.

CMV resistance of transgenic tobacco. *N. tabacum* is a native host of CMV. Typically, Q-CMV causes a chlorosis in the systemically infected leaves of the wild-type tobacco. SD-CMV and Fny-CMV-infected wild-type tobacco develops more pronounced disease symptoms, with striking chlorosis and curling in the systemically infected leaves (Fig. 6B, D, and F).

We first examined the Q-CMV resistance conferred by amiRNAs in the transgenic tobacco plants. Based on the resistance data from transgenic *Arabidopsis* plants, we chose amiR-SD-3, -2/3/5, and -1 transgenic tobacco lines, as well as amiR-Q-1 and -2 (designed for specific targeting of the Q-CMV 3′UTR) transgenic tobacco lines in the tests. T1 progeny derived from three independent primary transformants that expressed high levels of amiRNAs (Fig. 6A) were inoculated with sap extracted from Q-CMV-infected tobacco plants. Chlorosis appeared in upper noninoculated leaves at 6 dpi in all plants of the three amiR-SD-1 lines (lines 4, 5, and 6) and of two amiR-Q-1lines (lines 6 and 10) in 5 of 6 plants of the amiR-Q-1 line 1 and in 14 of 15 wild-type plants (Table 2 and Fig. 6B). A time course ELISA indicated that symptom development positively correlated with Q-CMV CP accumulation (Fig. 6H). High levels of the Q-CMV CP were observed in the amiR-Q-1 and amiR-SD-1 plants infected with Q-CMV, as well as in infected wild-type plants (Fig. 6C). These data suggest that neither amiR-Q-1 nor amiR-SD-1 can confer resistance to Q-CMV infection. In contrast, all of the inoculated plants of all three lines of amiR-Q-2 (lines 1, 2, and 3), amiR-SD-3 (lines 6, 15, and 18), and amiR-SD-2/3/5 (lines 1, 6, and 9) displayed normal appearance and undetectable Q-CMV CP

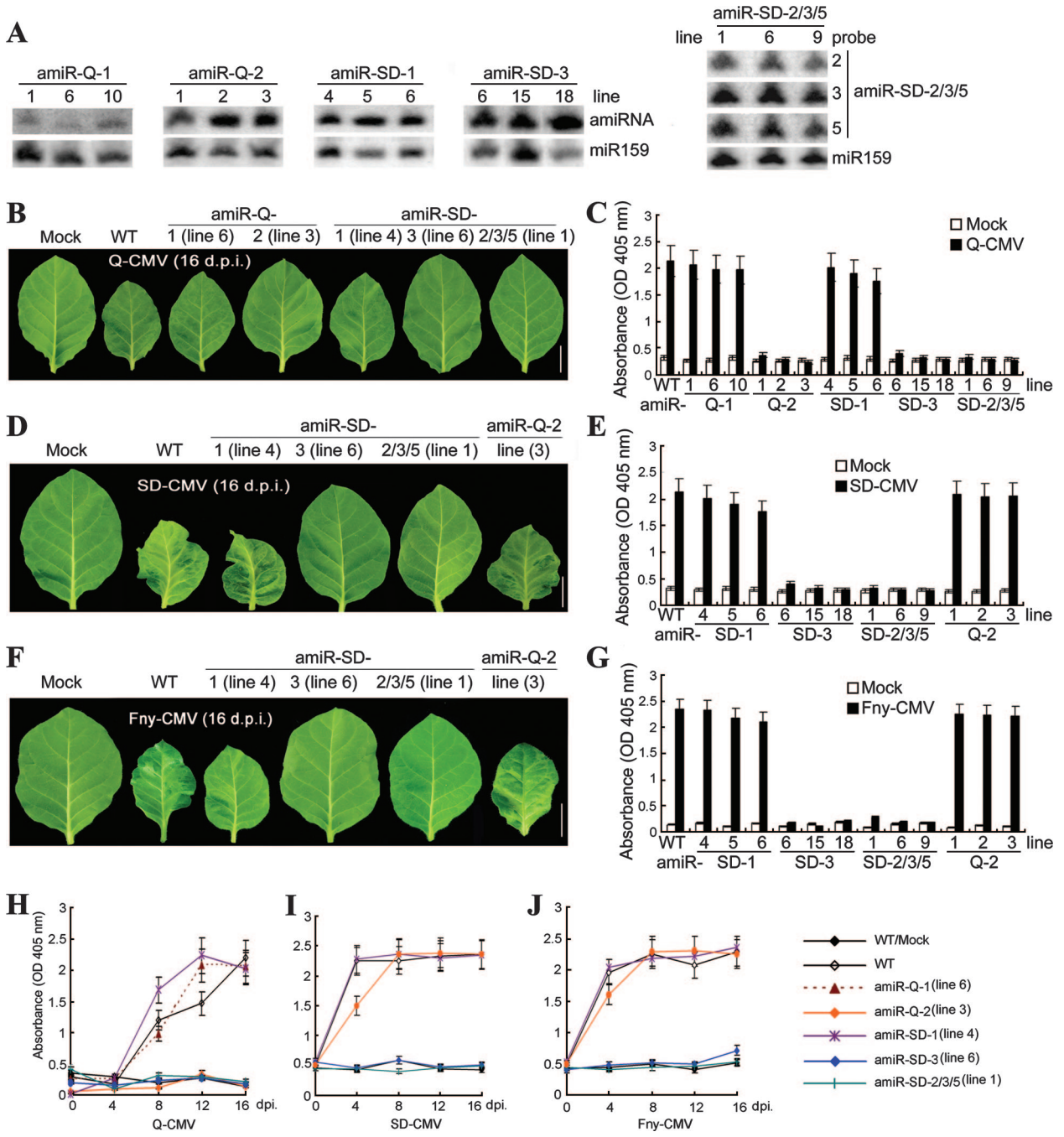

FIG. 6. amiRNA transgenic tobacco plants showed different resistances to Q-, SD-, and Fny-CMV infection. (A) Detection of amiRNA expression levels in the transgenic T1 progeny of each genotype. (B, D, and F) Plants were infected with Q-CMV (B), SD-CMV (D), or Fny-CMV (F), respectively. Photographs of systemic noninoculated leaves of representative line of each genotype are shown (16 dpi). Bar, 2 cm. (C, E, and G) ELISA detection of Q-CMV (C), SD-CMV (E), or Fny-CMV (G) CP in upper noninoculated leaves of three CMV strains or mock inoculation of each genotype plants at 16 dpi. Bars represent the standard deviations ($n = 6$). (H, I, and J) Time course analysis of CMV titer by ELISAs. Transgenic tobacco plants carrying 35S-amiR-SD-1, -3, and -2/3/5 and 35S-amiR-Q-1 and -2 T1 progeny and wild-type plants were inoculated by Q-CMV (H), SD-CMV (I), or Fny-CMV (J). Samples were collected from systemic noninoculated leaves of one representative line (as in panels B, D, and F) of each genotype and from wild-type plants at 0, 4, 8, 12, and 16 dpi. Readings were taken 1 h after substrate hydrolysis. Bars show standard deviations ($n = 5$).

(Fig. 6B and C). Similar results were obtained in a second experiment (Table 2).

We then examined SD-CMV resistance in the transgenic tobacco lines expressing of amiR-SD-1, -3, and -2/3/5 and amiR-Q-2. Typical chlorosis symptoms caused by SD-CMV appeared at 6 dpi in upper noninoculated leaves for all plants of the transgenic amiR-SD-1 lines (lines 4, 5, and 6) and in the wild-type plants in the two independent experiments (Table 3 and Fig. 6D), which is consistent with the results from *Arabidopsis* (Table 1). All plants from the amiR-Q-2 lines (lines 1, 2,

TABLE 2. Infectivity assay of amiRNA transgenic tobacco challenged with Q-CMV

Transgenic plant	Line	Infected/total inoculated plants[a]			
		Expt 1		Expt 2	
		I/T	R (%)	I/T	R (%)
amiR-Q-1	1	5/6	16.7	8/8	0
	6	6/6	0	8/8	0
	10	6/6	0	7/8	12.5
amiR-Q-2	1	0/6	100	0/8	100
	2	0/6	100	0/8	100
	3	0/6	100	1/8	87.5
amiR-SD-1	4	6/6	0	8/8	0
	5	6/6	0	8/8	0
	6	6/6	0	8/8	0
amiR-SD-3	6	0/6	100	1/10	90
	15	0/6	100	0/10	100
	18	0/6	100	0/10	100
amiR-SD-2/3/5	1	0/6	100	0/10	100
	6	0/6	100	0/9	100
	9	0/6	100	1/10	90
Wild type		14/15	6.7	12/12	0

[a] Tobacco wild-type plants and three independent lines of T1 progeny were challenged with Q-CMV in the two experiments. I/T and R are as described in Table 1.

and 3) were also fully sensitive to SD-CMV infection as expected, since there was no perfect targeting sequence in the SD-CMV 3′UTR for amiR-Q-2. ELISA detected similar accumulation levels of SD-CMV CP in the infected plants from each genotype (Fig. 6E and I). In contrast, all inoculated plants of the three amiR-SD-3 lines (lines 6, 15, and 18) and amiR-SD-2/3/5 lines (lines 1, 6, and 9) displayed normal appearance, like that of mock-inoculated plants (Fig. 6D), and SD-CMV CP was undetectable in these plants by ELISA (Fig. 6E). Similar results were obtained in a second experiment (Table 3). The percentages of resistance to SD-CMV infection in the two experiments ranged between 91.7 and 100% in the amiR-SD-3 lines and was 100% in the amiR-SD-2/3/5 lines (Table 3), a finding consistent with the results obtained for the amiR-SD-3 and -2/3/5 transgenic *Arabidopsis* strains (Table 1).

Resistance to Fny-CMV infection was also examined with the transgenic tobacco, and the data from two independent experiments are shown in Table 3. Due to the high similarity in the sequence of the 3′UTR region between SD- and Fny-CMV, which belong to the same subgroup of CMV, plants from the amiR-SD-3 and amiR-SD-2/3/5 cell lines, but not from the amiR-SD-1 and amiR-Q-2 transgenic lines, showed resistance to Fny-CMV infection (Fig. 6F), resembling the findings in the SD-CMV infection tests. ELISA confirmed the accumulation of Fny-CMV CP in the inoculated amiR-SD-1, amiR-Q-2, and wild-type plants and its absence in the asymptomatic inoculated amiR-SD-3 and amiR-SD-2/3/5 plants (Fig. 6G and J).

DISCUSSION

We show here that *Arabidopsis* and tobacco transgenic plants that express amiRNAs targeting the 3′UTR of CMV genomic RNA3 are not equally effective in conferring virus resistance because of extensive positional effects, such as the TLS structure in the 3′UTR region. Neither amiR-Q-1 nor amiR-SD-1, which has the target site located in the TLS region, conferred virus resistance. Our results for the biological function of amiR-Q-1 (Fig. 3) indicate that TLS structure impedes target site access and limits amiRNAs-RISC-mediated cleavage of the target viral RNA. Moreover, target recognition in the 5′ less-structured region of the 3′UTR, beyond the TLS, also influenced siRISC catalysis and resulted in conferring different degrees of resistance to CMV infection.

TABLE 3. Infectivity assay of amiRNA transgenic tobacco challenged with SD-CMV and Fny-CMV

Transgenic plant	Line	SD-CMV				FNY-CMV			
		Expt 1		Expt 2		Expt 1		Expt 2	
		I/T	R (%)	I/T	R (%)	I/T	R (%)	I/T	R (%)
amiR-SD-1	4	5/5	0	7/7	0	8/9	11.1	10/10	0
	5	5/5	0	7/7	0	9/9	0	9/10	10
	6	5/5	0	7/7	0	9/9	0	9/10	10
amiR-SD-3	6	0/6	100	0/12	100	0/12	100	1/10	90
	15	0/6	100	1/12	91.7	2/12	83.3	0/10	100
	18	0/6	100	1/12	91.7	0/12	100	1/10	90
amiR-SD-2/3/5	1	0/6	100	0/10	100	1/12	91.7	1/10	90
	6	0/6	100	0/10	100	0/12	100	0/10	100
	9	0/6	100	0/10	100	1/12	91.7	0/10	100
amiR-Q-2	1	5/5	0	8/8	0	12/12	0	10/10	0
	2	5/5	0	8/8	0	12/12	0	9/10	10
	3	5/5	0	8/8	0	10/12	16.7	10/10	0
Wild type		16/16	0	12/12	0	12/12	0	13/14	7.1

[a] Tobacco wild-type plants and three independent lines of T1 progeny were challenged with SD- and Fny-CMV in the two experiments. I/T and R are as described in Table 1.

Transgenic *Arabidopsis* plants carrying each of the three amiRNAs—amiR-SD-2, -3, and -5—that target the cleavage hotspots showed resistance to SD-CMV infection. Among the three amiRNAs, amiR-SD-3 seemed to be the best because both amiR-SD-3 transgenic *Arabidopsis* and tobacco plants had immunity to both subgroup strains of CMV. The amiR-SD-3-programmed RISC cleavage site was detected most frequently in the CMV-infected *dcl2/3/4* mutant. Together with the high efficacy of amiR-SD-3-mediated resistance to CMV infection, our results indicate that the amiR-SD-3 target site is a fully accessible RISC target site in the 3′UTR of CMV genome RNAs in natural infection conditions. We cannot clarify how vsiRNAs were produced in the *dcl2/3/4* mutant (Fig. 2C). It seems unlikely that the *dcl2/3/4* mutant contains the residual activity of DCL2, DCL3, or DCL4 because the triple *dcl* mutant was generated by standard genetic crosses using the three respective loss-of-function mutations, which are the T-DNA insertional mutations in *dcl2-1*, *dcl3-1*, and *dcl4-2* (21, 55). DCL1, on the other hand, has been shown to generate 21-nt siRNAs in the triple *dcl* mutant through hairpin RNA-mediated silencing constructs (16) and to generate 21-nt vsiRNAs in the triple *dcl* mutant that was infected with DNA viruses (6, 33). We speculate that, in the triple *dcl* mutant, the TLS region in the 3′UTR might be targeted by DCL1 or a DCL analog and that the resulting siRNAs in turn program the RISC cleavage where cleavage sites were mapped in the CMV-infected *dcl2/3/4* mutant (Fig. 2A). In fact, we found that some sequences in the TLS region potentially could form imperfect pairings with the 5′-terminal area of the 3′UTR. On the other hand, a low percentage of resistance to SD-CMV infection in the amiR-SD-4 plants was also correlated with the amiR-SD-4-mediated RISC cleavage site beyond the cleavage hot spot. There were no cleavage sites detected in the *dcl2/3/4* mutant within the amiR-SD-4 targeting area, suggesting that the target site is limited to target recognition and cleaved by siRISC, even though it is outside the TLS. The biological function of amiR-SD-4 was confirmed by using GUS-sensor construct via a transient system (data not shown). Therefore, the amiR-SD-4 target area may not be suitable for designing amiRNA to confer CMV resistance, even though the sequence is conserved in the 3′UTRs of all three CMV genomes.

In many plant viruses, sequence divergence is very high, and it may be difficult to select amiRNAs to target sequences that are conserved in most virus isolates. The lack of tools to accurately and reliably predict secondary structures within long RNAs makes it very hard to predict the secondary structures of a viral genome RNA in the natural infection conditions in vivo. Our work provides an experimental approach for analyzing the effects of target site accessibility on engineering effective virus resistance in plants by amiRNAs. By comparing the cleavage sites in the viral RNA of virus-infected wild-type and triple *dcl* mutant *Arabidopsis* plants, we can identify siRISC sensitive cleavage sites for the design of valid amiRNAs. The virus resistance levels conferred by amiRNAs that were designed from 5′RACE data suggest that our experimental approach is reliable. We cannot rule out that some mapped cleavage sites obtained from the triple mutant might be from random RNA degradation. However, a result obtained from the triple dcl mutant would reveal sites being cleaved more efficiently and possibly mediated by siRNA-RISC. Our results also suggest that 5′RACE data obtained from transient assays may not truly reflect natural conditions. Therefore, data from natural infections in vivo are required to draw confident conclusions.

We chose the CMV 3′UTR region as a target for amiRNA-mediated antiviral silencing for two reasons. First, the 3′UTR has a less-structured region at the 5′ terminus and a stable TLS structure at the 3′ terminus, which allowed us to examine whether target site accessibility influenced RISC catalysis in plants. Moreover, we also found that the target recognition was different in the 5′-terminal region. These observations, along with the highly conserved nucleotide sequence in the 3′UTR of all five genomic and subgenomic RNAs, including different subgroup strains of CMV, suggest that the 5′-terminal region of the 3′UTR still contains the conserved structures and/or sequences that are required for biological function. The requirement of conserved structures or sequences for biological function would restrict the viral RNAs from being mutated; therefore, target site selection based on this principle for amiRNA-mediated antiviral silencing may restrict the virus to evading the amiRNA surveillance mechanism and overcoming the specific resistance by mutations. The combination of the high specificity of miRNA cleavage and the high mutability of plant viruses makes it likely that resistance virus variants will emerge, as observed in plants infected with PPV chimeras bearing natural miRNA target sequence (46). We cannot rule out that the immunity of transgenic plants would not last under conditions of large-scale usage and high virus pressure. The polymer amiRNA strategy would be expected to resolve this problem. The polymer strategy is useful to express more than one kind of amiRNAs designed for different target RNAs to confer resistance to viruses, as previously reported by Niu et al. (34).

The second reason for choosing the 3′UTR region as the target is the highly conserved nucleotide sequence in all of the 3′UTR of five genomic and subgenomic RNAs of CMV. Cleavage of multiple CMV genome RNAs simultaneously may result in high resistance to CMV challenge. We obtained 83.3 to 100% resistance to both subgroup strains of CMV in the transgenic *Arabidopsis* and tobacco plants expressing amiRNAs targeting the 3′UTR region (Tables1, 2, and 3). In the previously reported amiR2b transgenic tobacco plants, ca. 63.6% (including "resistant," "recovery," and "delayed-infection" categories) of plants showed considerable resistance to SD-CMV infection (38). High resistance might be obtained by selection of optimal accessible target sites in the 2b sequence. However, the initially effective knockout of all of the target RNAs would protect the loading of amiRNAs into RISC from competition by vsiRNAs derived from the rapid replication of nontarget RNA1, -3, and -4 and thus maintain the abundance of amiRNA-RISC and target cleavage efficacy.

Plant miRNA-guided silencing has a widespread translational inhibitory component (7), and it might also have an effect on viral RNAs. We cannot rule out the possibility that translation inhibition has also contributed to the virus resistance observed in the plants expressing the 3′UTR-specific amiRNAs.

In conclusion, using an experimental approach with wild-type and RNA interference mutant plants to study the course of RISC target recognition on viral RNA in natural virus infection conditions, we can design 3′UTR-specific amiRNAs

that target fully accessible sites to obtain the highest effective resistance to CMV infection on amiRNA transgenic plants. The approach may be limited now to *Arabidopsis*, a plant of little agronomical interest, and viruses that can infect *Arabidopsis*. However, rapid developments in plant molecular biology and intensive research findings on RNA silencing in plants, for example, the *dcl* mutants in rice, are already available (28, 29), thus making it possible for this approach to have a broad application in the future. Moreover, the high conservation of the basic rules in miRNA biology also makes it likely that the information obtained from *Arabidopsis* will be useful for other plants. As in our case, amiRNAs designed based on the cleavage site analysis in SD-CMV-infected *Arabidopsis* have a similar effect in transgenic tobacco. We extrapolate that this experimental approach may also be adapted to animal systems in which RNAi mutant cell lines are available such as, for example, the *dcr-1 Drosophila* mutant (23), in order to apply amiRNAs in therapy.

ACKNOWLEDGMENTS

We thank Qi Xie for helpful comments and discussions and Steven E. Jacobsen for the *dcl2-1/3-1/4-2* mutant.

This research was supported by grants from the Ministry of Science and Technology of China, by the National Basic Research Program 973 (grant 2006CB101900), and by the National Science Foundation of China (grant 30771405 to H.-S.G. and grant 30530500 to R.-X.F.).

REFERENCES

1. **Alvarez, J. P., I. Pekker, A. Goldshmidt, E. Blum, Z. Amsellem, and Y. Eshed.** 2006. Endogenous and synthetic microRNAs stimulate simultaneous, efficient, and localized regulation of multiple targets in diverse species. Plant Cell **18:**1134–1151.
2. **Ameres, S. L., J. Martinez, and R. Schroeder.** 2007. Molecular basis for target RNA recognition and cleavage by human RISC. Cell **130:**101–112.
3. **Bartel, D. P.** 2004. MicroRNAs: genomics, biogenesis, mechanism, and function. Cell **116:**281–297.
4. **Baulcombe, D.** 2005. RNA silencing. Trends Biochem. Sci. **30:**290–293.
5. **Baulcombe, D.** 2004. RNA silencing in plants. Nature **431:**356–363.
6. **Blevins, T., R. Rajeswaran, P. V. Shivaprasad, D. Beknazariants, A. Si-Ammour, H. S. Park, F. Vazquez, D. Robertson, F. Meins, Jr., T. Hohn, and M. M. Pooggin.** 2006. Four plant Dicers mediate viral small RNA biogenesis and DNA virus induced silencing. Nucleic Acids Res. **34:**6233–6246.
7. **Brodersen, P., L. Sakvarelidze-Achard, M. Bruun-Rasmussen, P. Dunoyer, Y. Y. Yamamoto, L. Sieburth, and O. Voinnet.** 2008. Widespread translational inhibition by plant miRNAs and siRNAs. Science **30:**1185–1190.
8. **Brown, K. M., C. Y. Chu, and T. M. Rana.** 2005. Target accessibility dictates the potency of human RISC. Nat. Struct. Mol. Biol. **12:**469–470.
9. **Carrington, J. C., and V. Ambros.** 2003. Role of microRNAs in plant and animal development. Science **301:**336–338.
10. **Chen, Y. K., D. Lohuis, R. Goldbach, and M. Prins.** 2004. High frequency induction of RNA-mediated resistance against Cucumber mosaic virus using inverted repeat constructs. Mol. Breed. **14:**215–226.
11. **Clough, S. J., and A. F. Bent.** 1998. Floral dip: a simplified method for *Agrobacterium*-mediated transformation of *Arabidopsis thaliana*. Plant J. **16:** 735–743.
12. **Deleris, A., J. Gallego-Bartolome, J. Bao, K. D. Kasschau, J. C. Carrington, and O. Voinnet.** 2006. Hierarchical action and inhibition of plant Dicer-like proteins in antiviral defense. Science **313:**68–71.
13. **Ding, S. W., J. P. Rathjen, W. X. Li, R. Swanson, H. Healy, and R. H. Symons.** 1995. Efficient infection from cDNA clones of cucumber mosaic cucumovirus RNAs in a new plasmid vector. J. Gen. Virol. **76**(Pt. 2)**:**459–464.
14. **Du, Q. S., C. G. Duan, Z. H. Zhang, Y. Y. Fang, R. X. Fang, Q. Xie, and H. S. Guo.** 2007. DCL4 targets *Cucumber mosaic virus* satellite RNA at novel secondary structures. J. Virol. **81:**9142–9151.
15. **Fernandez-Cuartero, B., J. Burgyan, M. A. Aranda, K. Salanki, E. Moriones, and F. Garcia-Arenal.** 1994. Increase in the relative fitness of a plant virus RNA associated with its recombinant nature. Virology **203:**373–377.
16. **Fusaro, A. F., L. Matthew, N. A. Smith, S. J. Curtin, J. Dedic-Hagan, G. A. Ellacott, J. M. Watson, M. B. Wang, C. Brosnan, B. J. Carroll, and P. M. Waterhouse.** 2006. RNA interference-inducing hairpin RNAs in plants act through the viral defense pathway. EMBO Rep. **7:**1168–1175.
17. **Garcia, J. A., and C. Simon-Mateo.** 2006. A micropunch against plant viruses. Nat. Biotechnol. **24:**1358–1359.
18. **Guo, H. S., and J. A. Garcia.** 1997. Delayed resistance to *Plum pox potyvirus* mediated by a mutated RNA replicase gene: involvement of a gene-silencing mechanism. Mol. Plant-Microbe Interact. **10:**160–170.
19. **Guo, H. S., Q. Xie, J. F. Fei, and N. H. Chua.** 2005. MicroRNA directs mRNA cleavage of the transcription factor NAC1 to downregulate auxin signals for *Arabidopsis* lateral root development. Plant Cell **17:**1376–1386.
20. **Helliwell, C. A., and P. M. Waterhouse.** 2005. Constructs and methods for hairpin RNA-mediated gene silencing in plants. Methods Enzymol. **392:** 24–35.
21. **Henderson, I. R., X. Zhang, C. Lu, L. Johnson, B. C. Meyers, P. J. Green, and S. E. Jacobsen.** 2006. Dissecting *Arabidopsis* DICER function in small RNA processing, gene silencing, and DNA methylation patterning. Nat. Genet. **38:**721–725.
22. **Huesken, D., J. Lange, C. Mickanin, J. Weiler, F. Asselbergs, J. Warner, B. Meloon, S. Engel, A. Rosenberg, D. Cohen, M. Labow, M. Reinhardt, F. Natt, and J. Hall.** 2005. Design of a genome-wide siRNA library using an artificial neural network. Nat. Biotechnol. **23:**995–1001.
23. **Jin, Z., and T. Xie.** 2007. Dcr-1 maintains *Drosophila* ovarian stem cells. Curr. Biol. **17:**539–544.
24. **Khvorova, A., A. Reynolds, and S. D. Jayasena.** 2003. Functional siRNAs and miRNAs exhibit strand bias. Cell **115:**209–216.
25. **Kim, V. N.** 2005. MicroRNA biogenesis: coordinated cropping and dicing. Nat. Rev. Mol. Cell. Biol. **6:**376–385.
26. **Kwon, C. S., and W. I. Chung.** 2000. Differential roles of the 5′ untranslated regions of cucumber mosaic virus RNAs 1, 2, 3, and 4 in translational competition. Virus Res. **66:**175–185.
27. **Lindbo, J. A., L. Silva-Rosales, W. M. Proebsting, and W. G. Dougherty.** 1993. Induction of a highly specific antiviral state in transgenic plants: implications for regulation of gene expression and virus resistance. Plant Cell **5:**1749–1759.
28. **Liu, B., Z. Chen, X. Song, C. Liu, X. Cui, X. Zhao, J. Fang, W. Xu, H. Zhang, X. Wang, C. Chu, X. Deng, Y. Xue, and X. Cao.** 2007. Oryza sativa dicer-like4 reveals a key role for small interfering RNA silencing in plant development. Plant Cell **19:**2705–2718.
29. **Liu, B., P. Li, X. Li, C. Liu, S. Cao, C. Chu, and X. Cao.** 2005. Loss of function of OsDCL1 affects microRNA accumulation and causes developmental defects in rice. Plant Physiol. **139:**296–305.
30. **Llave, C., K. D. Kasschau, M. A. Rector, and J. C. Carrington.** 2002. Endogenous and silencing-associated small RNAs in plants. Plant Cell **14:**1605–1619.
31. **Luo, K. Q., and D. C. Chang.** 2004. The gene-silencing efficiency of siRNA is strongly dependent on the local structure of mRNA at the targeted region. Biochem. Biophys. Res. Commun. **318:**303–310.
32. **McManus, M. T., and P. A. Sharp.** 2002. Gene silencing in mammals by small interfering RNAs. Nat. Rev. Genet. **3:**737–747.
33. **Moissiard, G., and O. Voinnet.** 2006. RNA silencing of host transcripts by cauliflower mosaic virus requires coordinated action of the four *Arabidopsis* Dicer-like proteins. Proc. Natl. Acad. Sci. USA **103:**19593–19598.
34. **Niu, Q. W., S. S. Lin, J. L. Reyes, K. C. Chen, H. W. Wu, S. D. Yeh, and N. H. Chua.** 2006. Expression of artificial microRNAs in transgenic *Arabidopsis thaliana* confers virus resistance. Nat. Biotechnol. **24:**1420–1428.
35. **Ossowski, S., R. Schwab, and D. Weigel.** 2008. Gene silencing in plants using artificial microRNAs and other small RNAs. Plant J. **53:**674–690.
36. **Overhoff, M., M. Alken, R. K. Far, M. Lemaitre, B. Lebleu, G. Sczakiel, and I. Robbins.** 2005. Local RNA target structure influences siRNA efficacy: a systematic global analysis. J. Mol. Biol. **348:**871–881.
37. **Parizotto, E. A., P. Dunoyer, N. Rahm, C. Himber, and O. Voinnet.** 2004. In vivo investigation of the transcription, processing, endonucleolytic activity, and functional relevance of the spatial distribution of a plant miRNA. Genes Dev. **18:**2237–2242.
38. **Qu, J., J. Ye, and R. Fang.** 2007. Artificial microRNA-mediated virus resistance in plants. J. Virol. **81:**6690–6699.
39. **Reynolds, A., D. Leake, Q. Boese, S. Scaringe, W. S. Marshall, and A. Khvorova.** 2004. Rational siRNA design for RNA interference. Nat. Biotechnol. **22:**326–330.
40. **Rietveld, K., C. W. Pleij, and L. Bosch.** 1983. Three-dimensional models of the tRNA-like 3′ termini of some plant viral RNAs. EMBO J. **2:**1079–1085.
41. **Roossinck, M. J., L. Zhang, and K. H. Hellwald.** 1999. Rearrangements in the 5′ nontranslated region and phylogenetic analyses of cucumber mosaic virus RNA 3 indicate radial evolution of three subgroups. J. Virol. **73:**6752–6758.
42. **Schubert, S., A. Grunweller, V. A. Erdmann, and J. Kurreck.** 2005. Local RNA target structure influences siRNA efficacy: systematic analysis of intentionally designed binding regions. J. Mol. Biol. **348:**883–893.
43. **Schwab, R., S. Ossowski, M. Riester, N. Warthmann, and D. Weigel.** 2006. Highly specific gene silencing by artificial microRNAs in *Arabidopsis*. Plant Cell **18:**1121–1133.
44. **Schwarz, D. S., G. Hutvagner, T. Du, Z. Xu, N. Aronin, and P. D. Zamore.** 2003. Asymmetry in the assembly of the RNAi enzyme complex. Cell **115:** 199–208.
45. **Shao, Y., C. Y. Chan, A. Maliyekkel, C. E. Lawrence, I. B. Roninson, and Y.**

Ding. 2007. Effect of target secondary structure on RNAi efficiency. RNA **13:**1631–1640.
46. **Simon-Mateo, C., and J. A. Garcia.** 2006. MicroRNA-guided processing impairs *Plum pox virus* replication, but the virus readily evolves to escape this silencing mechanism. J. Virol. **80:**2429–2436.
47. **Smith, H. A., S. L. Swaney, T. D. Parks, E. A. Wernsman, and W. G. Dougherty.** 1994. Transgenic plant virus resistance mediated by untranslatable sense RNAs: expression, regulation, and fate of nonessential RNAs. Plant Cell **6:**1441–1453.
48. **Sugiyama, M., H. Sato, A. Katasawa, S. Hase, H. Takahashi, and Y. Ehara.** 2000. Characterization of symptom determinants in two mutants of cucumber mosaic virus Y strain, causing distinct mild green mosaic symptoms in tobacco. Physiol. Mol. Plant Pathol. **56:**85–90.
49. **Tuschl, T., P. D. Zamore, R. Lehmann, D. P. Bartel, and P. A. Sharp.** 1999. Targeted mRNA degradation by double-stranded RNA in vitro. Genes Dev. **13:**3191–3197.
50. **Vaucheret, H., F. Vazquez, P. Crete, and D. P. Bartel.** 2004. The action of Argonaute1 in the miRNA pathway and its regulation by the miRNA pathway are crucial for plant development. Genes Dev. **18:**1187–1197.
51. **Voinnet, O.** 2005. Induction and suppression of RNA silencing: insights from viral infections. Nat. Rev. Genet. **6:**206–220.
52. **Wang, J. W., L. J. Wang, Y. B. Mao, W. J. Cai, H. W. Xue, and X. Y. Chen.** 2005. Control of root cap formation by microRNA-targeted auxin response factors in *Arabidopsis*. Plant Cell **17:**2204–2216.
53. **Warthmann, N., H. Chen, S. Ossowski, D. Weigel, and P. Herve.** 2008. Highly specific gene silencing by artificial miRNAs in rice. PLoS ONE **3:**e1829.
54. **Waterhouse, P. M., M. W. Graham, and M. B. Wang.** 1998. Virus resistance and gene silencing in plants can be induced by simultaneous expression of sense and antisense RNA. Proc. Natl. Acad. Sci. USA **95:**13959–13964.
55. **Xie. Z., L. K. Johansen, A. M. Gustafson, K. D. Kasschau, A. D. Lellis, D. Zilberman, S. E. Jacobsen, and J. C. Carrington.** 2004. Genetic and functional diversification of small RNA pathways in plants. PLoS Biol. **2:**e104.
56. **Zamore, P. D., and B. Haley.** 2005. Ribo-gnome: the big world of small RNAs. Science **309:**1519–1524.
57. **Zamore, P. D., T. Tuschl, P. A. Sharp, and D. P. Bartel.** 2000. RNAi: double-stranded RNA directs the ATP-dependent cleavage of mRNA at 21 to 23 nucleotide intervals. Cell **101:**25–33.
58. **Zhang, Z. H., Q. Xie, and H. S. Guo.** 2007. Antiviral defense in plants. Plant Viruses **1:**21–26.